0026-895X/08/7303-686–696$20.00
MOLECULAR PHARMACOLOGY
Vol. 73, No. 3
41624/3304222
Mol Pharmacol 73:686–696, 2008
Printed in U.S.A.

A Three-Dimensional Quantitative Structure-Activity Analysis of a New Class of Bisphenol Topoisomerase IIα Inhibitors[S]

Hong Liang, Xing Wu, Jack C. Yalowich, and Brian B. Hasinoff

Faculty of Pharmacy, University of Manitoba, Winnipeg, Mannitoba, Canada (H.L., X.W., B.B.H.); and Department of Pharmacology, University of Pittsburgh School of Medicine, Pittsburgh, Pennsylvania (J.C.Y.)

Received September 10, 2007; accepted November 28, 2007

ABSTRACT

After the identification of a new lead bisphenol compound that had good topoisomerase IIα (EC 5.99.1.3) inhibitory activity, a series of bisphenol analogs were synthesized and tested to identify the structural features that were responsible for their activity. The bisphenols represent a new structural class of topoisomerase II inhibitor that potently inhibited the growth of Chinese hamster ovary and K562 leukemia cells in the low micromolar range. The fact that cell growth inhibition was significantly correlated with topoisomerase IIα inhibition suggests that the catalytic inhibition of topoisomerase IIα probably contributed to their growth inhibitory activity. Only one of the bisphenols (O3OH) tested significantly induced topoisomerase IIα-mediated cleavage of DNA. Most of the bisphenols displayed only low-fold cross-resistance to a K562 subline containing reduced levels of topoisomerase IIα Thus, it is likely that most of the bisphenols inhibited cell growth, not by acting as topoisomerase II poisons, but rather by acting as catalytic inhibitors of topoisomerase IIα. Three-dimensional quantitative structure-activity analysis (3D-QSAR) was carried out on the bisphenols using comparative molecular field analysis (CoMFA) and comparative molecular similarity index analysis (CoMSIA) to determine the structural features responsible for their activity. The CoMSIA analysis of the topoisomerase IIα inhibitory activity yielded a statistically significant model upon partial least-squares analyses. The 3D-QSAR CoMSIA analysis showed that polar meta hydrogen bond acceptor substituents on the phenyl rings favored inhibition of topoisomerase IIα. For the hydrogen bond donor field, *para*- and *meta*-substituted hydroxyl groups favored inhibition. Hydrophobic substituents on the bridge atoms disfavored inhibition.

Topoisomerase II (EC 5.99.1.3) alters DNA topology by catalyzing the passing of an intact DNA double helix through a transient double-stranded break made in a second helix, and it is critical for relieving torsional stress that occurs during replication and transcription and for daughter strand separation during mitosis (Fortune and Osheroff, 2000; Li and Liu, 2001; Wang, 2002). Mammalian cells contain α and β isoforms of topoisomerase II, with topoisomerase IIα being the most highly expressed in cells undergoing division (Akimitsu et al., 2003). Several widely used anticancer agents, including doxorubicin, daunorubicin (and other anthracyclines), amsacrine, etoposide, and mitoxantrone also target topoisomerase II, and they are thought to be cytotoxic because they are topoisomerase II poisons (Fortune and Osheroff, 2000; Li and Liu, 2001). Stabilization of the so called "cleavable complex" by topoisomerase II poisons increases the levels of protein-concealed DNA double-strand breaks in cells (Wilstermann and Osheroff, 2003). The action of DNA metabolic processes then transforms these complexes into permanent double-strand breaks, which are highly toxic to cells (Zhang et al., 1990).

In contrast, the catalytic inhibitors of topoisomerase II do not increase the levels of DNA breaks in cells at pharmacologically relevant concentrations. There are several classes of structurally unrelated catalytic inhibitors, including the bisdioxopiperazines [ICRF-187 (dexrazoxane), ICRF-193, and ICRF-154], the anthracycline derivative aclarubicin, merbarone, the quinobenzoxazines, and novobiocin (Hasinoff et al., 1995; Andoh and Ishida, 1998; Larsen et al., 2003). In this study, we report the discovery and synthesis of a new bisphenol class of topoisom-

This work was supported by the Canadian Institutes of Health Research; the Canada Research Chairs program; the Province of Manitoba, through the Manitoba Research and Innovation Fund; a Canada Research Chair in Drug Development (to B.B.H.); and by National Institutes of Health grant CA90787 (to J.C.Y.).
Article, publication date, and citation information can be found at http://molpharm.aspetjournals.org.
doi:10.1124/mol.107.041624.
[S] The online version of this article (available at http://molpharm.aspetjournals.org) contains supplemental material.

ABBREVIATIONS: kDNA, kinetoplast DNA; MTS, 3-(4,5-dimethylthiazol-2-yl)-5-(3-carboxymethoxyphenyl)-2-(4-sulfophenyl)-2*H*-tetrazolium, inner salt; CHO, Chinese hamster ovary; ΔT_m, change in the DNA thermal melt temperature; CoMFA, comparative molecular field analysis; CoMSIA, comparative molecular similarity index analysis; 3D, three-dimensional; QSAR, quantitative structure-activity relationship; LOO, leave-one-out; RR, relative resistance.

erase II inhibitors. A lead bisphenol analog was obtained subsequent to screening compounds from the National Cancer Institute for the inhibition of the decatenation activity of topoisomerase IIα. Several of these bisphenols showed submicromolar inhibition of the decatenation activity of topoisomerase IIα. Only one of the bisphenols tested increased the levels of topoisomerase IIα-DNA covalent complexes, which suggests that these compounds largely inhibited cell growth by acting as catalytic inhibitors of topoisomerase II. The topoisomerase IIα inhibitory activity of the bisphenols were analyzed using 3D-QSAR modeling methods to identify the structural features responsible for their activity.

Materials and Methods

Materials and Synthesis of Bisphenols. pBR322 plasmid DNA was obtained from MBI Fermentas (Burlington, ON, Canada), and the kDNA was from TopoGEN, Inc. (Columbus, OH). HindIII was from Invitrogen (Burlington, ON, Canada). Unless indicated, other chemicals were from Sigma-Aldrich (Oakville, ON, Canada). The MTS CellTiter 96 AQueous One Solution Cell Proliferation Assay kit was obtained from Promega (San Luis Obispo, CA). The structures of the compounds tested are shown in Fig. 1. DHDPS1, DHPDS2, SCHO1, SCHO2, OCHO1, OCHO2, S3OH, S4OH, O3OH, bisAC3, bispCP5, and cyclofenil diphenol were synthesized and characterized by ^{1}H and ^{13}C nuclear magnetic resonance spectroscopy and electrospray ionization mass spectrometry as described in Supplemental Material. Of these compounds, OCHO1 and S3OH have not been described previously. DHDP, TDP, EIBP, BHPM, and 4,4′-dihydroxybenzophenone were purchased from Sigma-Aldrich, and the NSC-labeled[1] compounds were obtained from the National Cancer Institute (Bethesda, MD). The linear and nonlinear least-squares analyses were done with SigmaStat (Systat Software, Inc., Point Richmond, CA). The error bars shown are ± S.E.M.

Cell Culture and Growth Inhibition Assays. Human leukemia K562 cells, obtained from the American Type Culture Collection and K/VP.5 cells (a 26-fold etoposide-resistant K562-derived subline with decreased levels of topoisomerase IIα and topoisomerase IIβ mRNA and protein) (Ritke et al., 1994b) were maintained as suspension cultures in Dulbecco's modified Eagle's medium (Invitrogen) containing 4 mM L-glutamine and supplemented with 20 mM HEPES (Sigma-Aldrich, St. Louis, MO), 10% fetal calf serum (Invitrogen), 100 units/ml penicillin G, and 100 μg/ml streptomycin in an atmosphere of 5% CO_2 and 95% air at 37°C, pH 7.4. The spectrophotometric 96-well plate cell growth inhibition MTS assay, which measures the ability of the cells to enzymatically reduce MTS after drug treatment, has been described previously (Liang et al., 2006). The drugs were dissolved in dimethyl sulfoxide. The final concentration of dimethyl sulfoxide did not exceed 0.5% (v/v), and it was an amount that had no detectable effect on cell growth. The cells were incubated with the drugs for the times indicated and then assayed with MTS. IC_{50} values for growth inhibition in both assays were measured by fitting the absorbance-drug concentration data to a four-parameter logistic equation as described previously (Liang et al., 2006). Typically, 10 different concentrations were used in the nonlinear least-squares analysis to construct the dose-response curves and to obtain the IC_{50} values. For 15 of the 23 bisphenol compounds, IC_{50} values for K562 growth inhibition were obtained from averaging experiments that were run two to four times on a different days. CHO cells (type AA8; ATCC CRL-1859), obtained from the American Type Culture Collection (Manassas, VA) and DZR cells (a dexrazoxane-resistant CHO cell line we described previously) (Hasinoff et al., 1997; Wu and Hasinoff, 2005) were grown in α minimal essential medium (Invitrogen) containing 20 mM HEPES, pH 7.4, and they were assayed for their growth inhibitory effects using the 3-(4,5-dimethylthiazol-2-yl)-2,5-diphenyltetrazolium assay as described previously (Hasinoff et al., 2004).

[1] The structure and the names of all the National Cancer Institute NSC numbered compounds used in this study can be found at http://129.43.27.140/ncidb2/.

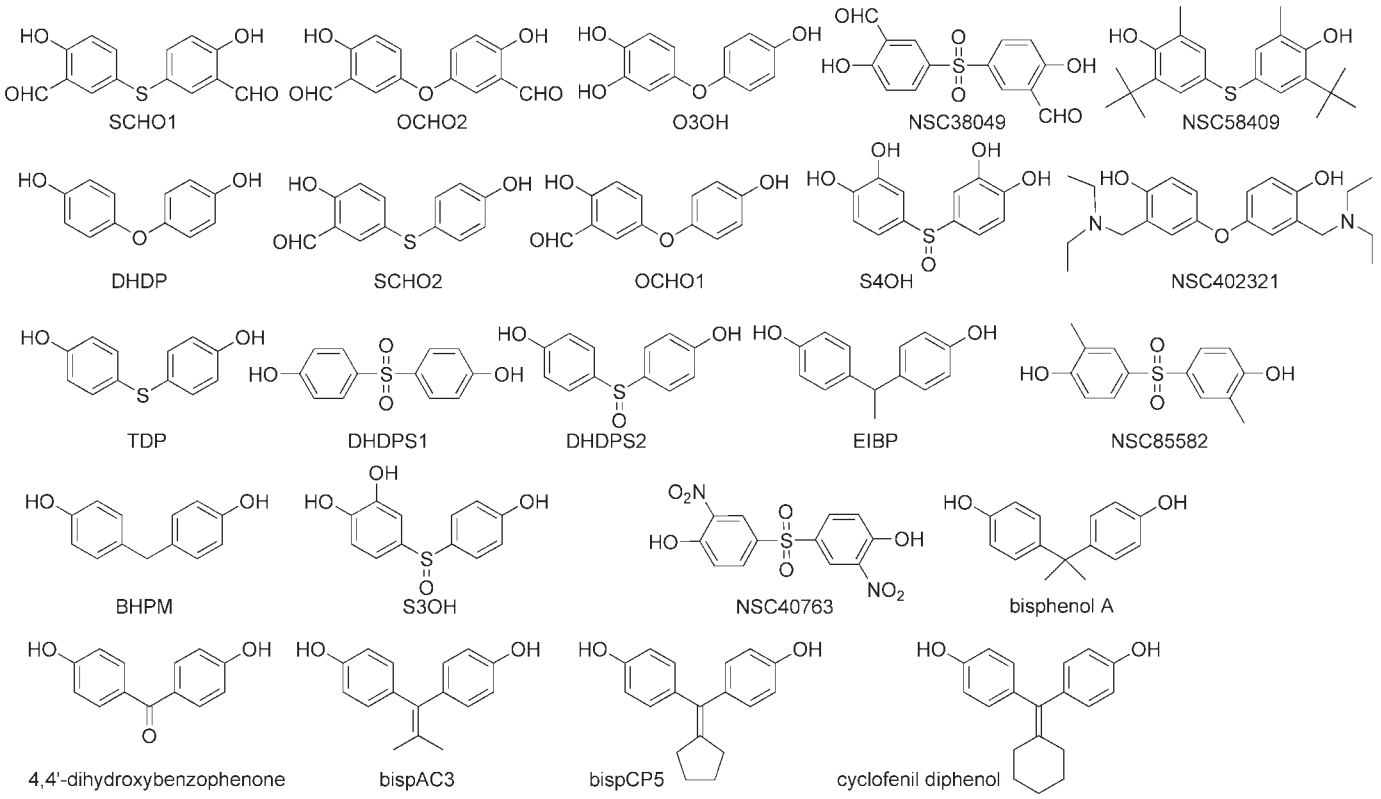

Fig. 1. Structures of the bisphenols tested for inhibition of topoisomerase IIα and inhibition of cell growth.

Topoisomerase IIα kDNA Decatenation Inhibition Assay. A spectrofluorometric decatenation assay was used to determine the inhibition of topoisomerase IIα by the bisphenols (Hasinoff et al., 2004, 2005; Liang et al., 2006). kDNA consists of highly catenated networks of circular DNA. Topoisomerase IIα decatenates kDNA in an ATP-dependent reaction to yield individual minicircles of DNA. The 20-μl reaction mixture contained 0.5 mM ATP, 50 mM Tris-HCl, pH 8.0, 120 mM KCl, 10 mM $MgCl_2$, 30 μg/ml bovine serum albumin, 50 ng of kDNA, test compound (0.5 μl in dimethyl sulfoxide), and 20 ng of topoisomerase IIα protein (the amount that gave approximately 80% decatenation). Using a high-copy yeast expression vector, full-length human topoisomerase IIα was expressed, extracted, and purified as described previously (Hasinoff et al., 2005). The final dimethyl sulfoxide concentration of 2.5% (v/v) was shown in controls not to affect the activity of topoisomerase IIα. The assay incubation was carried out at 37°C for 20 min, and it was terminated by the addition of 12 μl of 250 mM Na_2EDTA. Samples were centrifuged at 8000*g* at 25°C for 15 min, and 20 μl of the supernatant was added to 180 μl of 600-fold diluted PicoGreen dye (Molecular Probes, Eugene, OR) in a 96-well plate. The fluorescence, which was proportional to the amount of kDNA, was measured in a Fluostar Galaxy (BMG, Durham, NC) fluorescence plate reader using an excitation wavelength of 485 nm and an emission wavelength of 520 nm. IC_{50} values for inhibition of topoisomerase IIα decatenation activity were measured by fitting the fluorescence-drug concentration data to a four-parameter logistic equation as described previously (Liang et al., 2006). Typically, 10 different concentrations were used in the nonlinear least-squares analysis to construct the dose-response curves and to obtain the IC_{50} values.

Topoisomerase I pBR322 DNA Relaxation Inhibition Assay. A gel assay was used to determine whether the bisphenols inhibited topoisomerase I. The recombinant human topoisomerase I, pBR322 DNA, and assay buffer were from TopoGEN, Inc. The 20-μl assay mixture contained 50 ng of pBR322 DNA, 0.5 units of topoisomerase I, and 10 μM test drugs. After 30-min incubation at 37°C in assay buffer, the reaction was terminated with 0.5% (v/v) SDS and 25 mM Na_2EDTA. Electrophoresis was carried out as described for the topoisomerase IIα cleavage assay below, except that neither the gel nor the running buffer contained ethidium bromide, to obtain good separation of the relaxed and supercoiled DNA. In the absence of ethidium bromide, the supercoiled DNA runs ahead of the relaxed DNA.

pBR322 DNA Cleavage Assays. Topoisomerase II-cleaved DNA complexes produced by anticancer drugs may be trapped by rapidly denaturing the complexed enzyme with SDS (Burden et al., 2001; Liang et al., 2006). The drug-induced cleavage of double-stranded closed circular pBR322 DNA to form linear DNA was followed by separating the SDS-treated reaction products using ethidium bromide gel electrophoresis as described previously (Burden et al., 2001; Liang et al., 2006). The 20-μl cleavage assay reaction mixture contained 100 μM drug, 150 ng of topoisomerase IIα protein, 80 ng of pBR322 plasmid DNA (MBI Fermentas), 0.5 mM ATP in assay buffer [10 mM Tris-HCl, 50 mM KCl, 50 mM NaCl, 0.1 mM EDTA, 5 mM $MgCl_2$, 2.5% (v/v) glycerol, pH 8.0, and drug (0.5 μl in dimethyl sulfoxide)]. The order of addition was assay buffer, DNA, drug, and then topoisomerase IIα. The reaction mixture was incubated at 37°C for 10 min, and it was quenched with 1% (v/v) SDS and 25 mM Na_2EDTA. The reaction mixture was treated with 0.25 mg/ml proteinase K (Sigma-Aldrich) at 55°C for 30 min to digest the protein. The linear pBR322 DNA cleaved by topoisomerase IIα was separated by electrophoresis (1 h at 8 V/cm and then 15 h at 1 V/cm to obtain good separation of the supercoiled and relaxed DNA) on a 4 mM Tris base/0.11% (v/v) glacial acetic acid/2 mM Na_2EDTA buffer/0.5 μg/ml ethidium bromide/1.2% (w/v) agarose gel. The DNA in the gel was imaged by its fluorescence on an Alpha Innotech (San Leandro, CA) Fluorochem 8900 imaging system equipped with a 365-nm UV illuminator and a charge-coupled device camera.

Thermal Denaturation of DNA Assay. Compounds that intercalate into DNA stabilize the DNA double helix and increase the temperature at which the DNA is denatured (Priebe et al., 2001). The effect of 2 μM concentrations of the compounds on the change in the DNA thermal melt temperature (ΔT_m) of sonicated calf thymus DNA (5 μg/ml) was measured in 10 mM Tris-HCl buffer, pH 7.5, in a Cary 1 (Varian, Mississauga, ON, Canada) double-beam spectrophotometer by measuring the absorbance increase at 260 nm upon the application of a temperature ramp of 1°C/min. The maximum of the first derivative of the absorbance-temperature curve was used to obtain the ΔT_m. Doxorubicin (2 μM), which is a strong DNA intercalator, was used as a positive control (Priebe et al., 2001).

Modeling and Conformation Search. All molecular modeling was done using SYBYL 7.2.3 (Tripos, St. Louis, MO) on an XW4100 PC workstation (Hewlett Packard, Palo Alto, CA), with a Redhat Enterprise 3 Linux operating system. All molecules were built using SYBYL. Geometry optimization was carried out with the Tripos force field using a conjugate gradient with a convergence criterion of 0.01 kcal/mol and Gasteiger-Huckel charges and a distance-dependent dielectric constant.

Three-Dimensional Quantitative Structure-Activity Analyses. The CoMFA and CoMSIA analyses require that the 3D structures of the molecules be aligned to a core conformational template that is their presumed active form (Cramer et al., 1988; Klebe et al., 1994; Kubinyi et al., 1998). For the CoMFA analysis, steric and electrostatic field energies were calculated using an sp^3 carbon with a van der Waals radius of 1.52 Å as the steric probe and a +1 charge as an electrostatic probe. Steric and electrostatic interactions were calculated using the Tripos force field with a distance-dependent dielectric constant at all lattice points of a regular-spaced (2-Å) grid. The energy cut-off was 30 kcal/mol. The alignment and lattice box used for the CoMFA calculation were also used to calculate similarity index fields for the CoMSIA analysis. Steric, electrostatic, hydrophobic, and hydrogen bond donor and acceptor fields were evaluated in the CoMSIA analysis. Similarity indices were computed using a probe atom with a +1 charge, radius of 1 Å, hydrophobicity of +1, hydrogen bond donating of +1, hydrogen bond acceptor of +1, and attenuation factor α of 0.3 for the Gaussian-type distance. A partial least-squares statistical approach, which is an extension of multiple regression analysis in which the original variables are replaced by a set of their linear combinations, was used to obtain the 3D-QSAR results. All models were investigated using the leave-one-out (LOO) method, which is a cross-validated partial least-squares method. The CoMFA and CoMSIA descriptors were used as independent variables, and the pIC_{50} value was used as the dependent variable to derive the 3D-QSAR models. The cross-validated correlation coefficient q^2 and the optimum number of components (N) were obtained by the LOO method. The final model (non–cross-validated conventional analysis) was developed and yielded the non–cross-validated correlation coefficient r^2, with the optimum number of components.

Results

Effect of Bisphenols on Thermal Denaturation of DNA. Doxorubicin (2 μM), which is a well known DNA-intercalating drug (Priebe et al., 2001), was used as a control, and it was observed to increase the ΔT_m of sonicated DNA by 13.2°C from 71.0°C. The following compounds were tested at 2 μM to see whether they affected the ΔT_m: NSC38049, NSC85582, NSC402321, DHDP, NSC58409, SCHO1, SCHO2, TDP, BHPM, and EIBP. None of these compounds significantly changed the ΔT_m (data not shown); thus, it can be concluded that they did not act, at least at the concentrations tested, by binding to DNA.

Effect of Bisphenols on K562 Cell Growth Inhibition. Examples of the growth inhibitory effects of the bisphenols

S4OH and DHDP on K562 cells are shown in Fig. 2A. The IC_{50} data for the growth inhibitory effects of all the bisphenols tested on K562 and K/VP.5 cells are given in Table 1. It can be seen from the data in Table 1 from a comparison of the structure of DHDP with the 4,4′-bisphenol analogs TDP, BHPM, EIBP, DHDS2, and DHDS1 that an electronegative atom, such as sulfur or oxygen, in the bridge between the phenyl rings increased growth inhibitory activity compared with a CH_2 or $CHCH_3$ bridge (IC_{50} values: DHDP < TDP < EIBP < BHPM). Further substitution of the carbon linker (as in bisphenol A) or conversion of the methyl-substituted carbon linker in BHPM into either a ketone (4,4′-dihydroxybenzophenone) or double-bonded conjugates (bispAC3, bispCP5, or cyclofenil diphenol) had little positive effect on activity. Conversion of the sulfur in TDP to a sulfone or sulfoxide also decreased activity. A comparison of the sulfones S4OH, DHDPS2, and S3OH indicated that electron donor groups at the 3,3′ positions increased activity (IC_{50} values: S4OH < S3OH < DHDPS2).

Bisphenols Inhibited the Decatenation Activity of Topoisomerase IIα but Did Not Inhibit the Relaxation Activity of Topoisomerase I. As shown in Fig. 2B for S4OH and DHDP specifically, and in Table 1 for all compounds tested, the bisphenols varied considerably in their ability to inhibit decatenation activity of human topoisomerase IIα. This assay is a measure of the inhibition of catalytic enzyme activity only, and it is not a measure of whether these compounds acted as topoisomerase II poisons as do some widely used anticancer drugs (Fortune and Osheroff, 2000; Li and Liu, 2001). The activity of the sulfoxide S4OH was close in activity to the oxygen-ether O3OH. An electronegative atom such as a sulfoxide (as in S4OH) or an oxygen (as in O3OH) or sulfur (as in SCHO1 OR SCHO2) in the bridge between the phenyl rings increased topoisomerase IIα inhibitory activity compared with a CH_2 bridge (BHPM). Substitution of the 3-position in the oxygen-ether DHDP with a single OH (as in O3OH) increased activity, whereas replacement at the 3- or 3′-OH with one or two formyl groups decreased activity (OCHO1 and OCHO2, respectively). Conversely, when TDP with a sulfur-ether was modified with the addition of either one or two formyl groups (SCHO2 and SCHO1, respectively) activity was increased. The most potent topoisomerase IIα inhibitor, the biscatechol sulfoxide S4OH, was also more potent than S3OH, indicating a preference for 3,3′-electronegative substitution. The two sulfones tested NSC38049 and NSC40763 were of lower activity, suggesting a sulfoxide (or a sulfur or oxygen) was more favorable for activity. As with K562 cell growth inhibitory activity, further substitution or conversion of the linker in EIBP (as in bisphenol A; 4,4′-dihydroxybenzophenone; bispAC3; bispCP5; or cyclofenil diphenol) did not improve activity.

Experiments to determine whether the bisphenols had

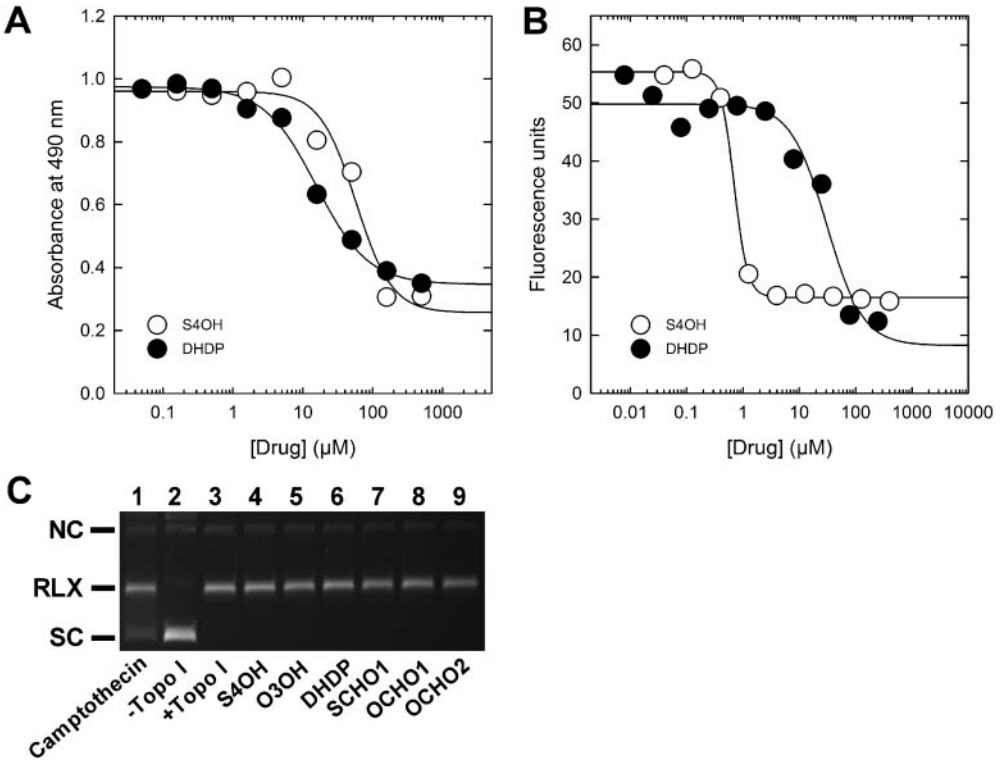

Fig. 2. Bisphenols inhibit K562 cell growth and the catalytic decatenation activity of topoisomerase IIα, but they do not inhibit the relaxation activity of topoisomerase I. A, inhibition of growth of K562 cells by S4OH (○) and DHDP (●). Cells were treated with the bisphenol indicated for 72 h before assessment of growth inhibition by an MTS assay. The curved solid lines are nonlinear least-squares fits to a four-parameter logistic equation, and they yield IC_{50} values of 64 ± 24 and 9.7 ± 5.5 μM, respectively, for S4OH and DHDP. B, inhibition of the catalytic decatenation activity of topoisomerase IIα by S4OH (○) and DHDP (●). The curved solid lines are nonlinear least-squares fits to a four-parameter logistic equation, and they yield IC_{50} values of 0.69 ± 0.07 and 31 ± 12 μM, respectively, for S4OH and DHDP. C, effects of bisphenols and camptothecin on the ability of topoisomerase I to relax supercoiled pBR322 DNA. This fluorescent image of the ethidium bromide-stained gel shows that the bisphenols did not detectably inhibit the relaxation activity of topoisomerase I, whereas the topoisomerase I inhibitor camptothecin did (lane 1). All lanes except lane 2 contained topoisomerase I. All drugs, where indicated, were present at a concentration of 10 μM in the assay mixture. In this gel, which was stained with ethidium bromide after it was run, the supercoiled DNA (SC) ran ahead of the relaxed DNA (RLX). A small amount of nicked circular (NC) is normally seen in pBR322 DNA.

specificity for inhibition of topoisomerase IIα were carried out using topoisomerase I, which is a DNA-processing enzyme (Pommier et al., 1998) that also relieves torsional stress in DNA. Topoisomerase I relaxes DNA through a transient single-strand break in DNA compared with the transient double-strand break in DNA induced by topoisomerase II (Pommier et al., 1998). As shown by the gel in Fig. 2C S4OH, O3OH, DHDP, SCHO1, OCHO1, and OCHO2 did not detectably inhibit the relaxation activity of topoisomerase I toward supercoiled pBR322 DNA, whereas the well known topoisomerase I inhibitor camptothecin did (Pommier et al., 1998).

QSAR Correlation Analyses of CHO on K562 Cell Growth Inhibition with Topoisomerase IIα Inhibition. As shown in Fig. 3, A and B, the logarithms of the CHO and K562 IC_{50} data were significantly correlated with the logarithm of the IC_{50} data for the catalytic inhibition of topoisomerase IIα ($r^2 = 0.56$, $p < 0.001$ and $r^2 = 0.24$, $p = 0.02$, respectively). The significant correlation of the CHO and K562 IC_{50} data with topoisomerase IIα IC_{50} suggests that inhibition of topoisomerase IIα by the bisphenols contributed to the inhibition of cell growth.

Effect of Bisphenols on Stabilization of the Covalent Topoisomerase IIα-DNA Cleavable Complex. Several widely used anticancer agents, including doxorubicin and the other anthracyclines, mitoxantrone, and etoposide (Fortune and Osheroff, 2000; Li and Liu, 2001), are thought to be cytotoxic by virtue of their ability to stabilize a covalent topoisomerase II-DNA intermediate (the cleavable complex), thereby acting as topoisomerase II poisons. Thus, DNA cleavage assay experiments (Burden et al., 2001) were carried out as we described previously (Hasinoff et al., 2006), using etoposide as a positive control to see whether 250 μM concentrations of the test compounds stabilized the cleavable complex to produce linear DNA. As shown in Fig. 4, A and B, the addition of 250 μM etoposide (lane 3) to the reaction mixture containing topoisomerase IIα and supercoiled pBR322 DNA significantly ($p < 0.01$) induced formation of linear DNA 2.6-fold compared with background levels in the absence of topoisomerase IIα. Linear DNA was identified by comparison with linear pBR322 DNA produced by action of the restriction enzyme HindIII acting on a single site on pBR322 DNA (data not shown). O3OH also significantly ($p < 0.001$) increased formation of linear DNA an average of 1.8-fold over background levels. However, as determined by *t* test, none of the other bisphenols shown in Fig. 4, A and B (S4OH, DHDP, or SCHO1), statistically significantly increased formation of linear DNA over background levels. OCHO1, OCHO2, SCHO2, NSC402321, and NSC40763 were also tested, and they gave similar negative results. These results indicate that only O3OH of the bisphenols tested acted as a topoisomerase IIα poison.

As exemplified by dexrazoxane (Fattman et al., 1996; Hasinoff et al., 1997), catalytic inhibitors of topoisomerase II may inhibit cleavable complex formation by topoisomerase II poisons such as etoposide (Andoh and Ishida, 1998; Larsen et al., 2003; Jensen et al., 2005; Jensen et al., 2006). Experiments were thus carried out to see whether bisphenol pretreatment could antagonize etoposide-induced linear DNA formation by topoisomerase IIα. As the results in Fig. 4, C and D show, S4OH, O3OH, DHDP, and SCHO1 all reduced the amount of linear DNA produced from etoposide-induced formation of the cleavable complex. SCHO1 decreased the average amount of etoposide-induced linear DNA formation the most (from 1.9- to 1.5-fold over no-drug control levels). However, there was no statistically significant bisphenol-

TABLE 1

Cell growth inhibitory and topoisomerase II inhibitory effects of the bisphenols

The relative resistance (RR) factors were calculated from the ratio of the IC_{50} value for the K/VP0.5 cell line divided by that for the K562 cell line or the DZR to the CHO cell line, respectively.

Compound or NSC No.	MTS Cell Growth Inhibition			MTT Cell Growth Inhibition			Topoisomerase IIα Inhibition, IC_{50}
	IC_{50}		RR	IC_{50}		RR	
	K562	K/VP0.5		CHO	DZR		
	μM			μM			μM
SCHO1	6.2	5.9	0.96	11	20	1.89	7.8
OCHO2	8.9	2.6	0.29	18	24	1.34	44
O3OH	9.3	15	1.61	13	14	1.04	0.74
DHDP	9.7	32	3.28	13	13	1.02	31
NSC38049	21	26	1.26	50	41	0.82	252
NSC58409	24	24	1.00	9.2	21	2.27	585
TDP	33	68	2.08	171	127	0.74	326
SCHO2	51	50	0.99	39	104	2.64	18
OCHO1	54	32	0.59	36	27	0.73	26
BispCP5	55	56	1.02	63	145	2.30	110
NSC402321	63	94	1.49	133	115	0.86	640
S4OH	64	26	0.41	10	8.6	0.83	0.69
Cyclofenil diphenol	71	66	0.93	64	83	1.30	511
BispAC3	72	79	1.10	77	90	1.17	201
EIBP	82	73	0.90	276	169	0.61	1640
Bisphenol A	96	122	1.27	124	187	1.51	501
4,4′-Dihydroxybenzophenone	99	146	1.47	171	194	1.13	483
NSC85582	117	73	0.63	218	151	0.69	571
BHPM	134	198	1.48	361	298	0.83	1011
DHDPS1	143	313	2.19	396	186	0.47	487
S3OH	143	223	1.56	61	42	0.69	133
DHDPS2	182	355	1.95	>1000	685	N.D.	>1000
NSC40763	525	251	0.48	96	71	0.74	135

N.D., not determined.

induced decrease in linear DNA compared with the etoposide-treated control for any of the bisphenols tested.

Effect of Bisphenols on the Growth of a K562 Cell Line Compared with the K/VP.5 Cell Line with a Decreased Level of Topoisomerase IIα. One method by which cancer cells increase their resistance to topoisomerase II poisons is by lowering their level or activity of topoisomerase II (Ritke et al., 1994a,b; Fortune and Osheroff, 2000). With less topoisomerase II in the cell, cells produce fewer DNA strand breaks, and topoisomerase II poisons are less lethal to cells. These cell lines provide a convenient way to test whether a drug that inhibits topoisomerase II acts as a topoisomerase II poison (Hasinoff et al., 2005). Conversely, a lack of change in sensitivity of a putative topoisomerase II poison to a cell line with a lowered topoisomerase II level can be taken to indicate that poisoning of topoisomerase II was not an important mechanism for this particular agent. We previously reported that topoisomerase IIα and topoisomerase IIβ protein levels were reduced 6- and 3-fold, respectively, in K/VP.5 compared with K562 cells (Ritke et al., 1994b). A 72-h continuous treatment with a range of concentrations of the bisphenols was used to generate IC_{50} values for growth inhibition in K562 and K/VP.5 cells, as measured with the MTS assay (Table 1). None of the bisphenols were very cross-resistant, which again suggests that the bisphenols inhibited cell growth mainly through the catalytic inhibition of topoisomerase II.

Because the bisphenols display some structural resemblance to the bisdioxopiperazine dexrazoxane (ICRF-187) in that both have bis-substituted ring systems joined by linker atoms, we also determined the ability of the bisphenols to inhibit the growth of our previously characterized dexrazoxane-resistant DZR cell line (Hasinoff et al., 1997, 2004; Wu and Hasinoff, 2005). The DZR cell line, which was derived from the parent CHO cell line and has a Thr48Ile mutation in topoisomerase IIα, is 400-fold resistant to dexrazoxane (Hasinoff et al., 1997; Hasinoff et al., 2004; Wu and Hasinoff, 2005). This mutation is located in the N-terminal ATP binding region of topoisomerase II close to the dexrazoxane binding site (Classen et al., 2003), and it probably interferes with dexrazoxane binding. The results in Table 1 show that none of the bisphenols were greater than 2.6-fold cross-resistant to the DZR cell line, which indicates that the bisphenols did not inhibit the catalytic activity of topoisomerase IIα by binding to the bisdioxopiperazine binding site.

Effect of Bisphenols on the K562 Cell Growth Inhibitory Effects of the Topoisomerase II Poisons Doxorubicin and Etoposide. We and others have shown that the bisdioxopiperazine topoisomerase II catalytic inhibitors dexrazoxane and ICRF-193 antagonized the growth inhibitory effects of doxorubicin, daunorubicin, etoposide, and amsacrine (Ishida et al., 1991; Tanabe et al., 1991; Sehested et al., 1993; Hasinoff et al., 1996). Likewise, the purine NSC35866 (Jensen et al., 2005) can antagonize etoposide-induced growth inhibitory effects. For dexrazoxane, it may do this by trapping the enzyme in the form of a closed protein clamp, thereby preventing the formation or stabilization of the topoisomerase II-DNA intermediate (Ishida et al., 1991; Tanabe et al., 1991; Sehested et al., 1993).

To determine whether the bisphenols acted similarly to dexrazoxane (Hasinoff et al., 1996) and NSC35866 (Jensen et al., 2005) in antagonizing doxorubicin or etoposide growth inhibitory effects on K562 cells, experiments were carried out in which K562 cells were pretreated with either 5 μM O3OH or S4OH for 30 min before treatment with doxorubicin (Fig. 5, A and B) and then continuously incubated with both drugs for 72 h before the MTS assay. These concentrations of O3OH or S4OH are approximately 6-fold higher than that required to inhibit the catalytic activity of topoisomerase IIα (Table 1), but were not high enough to significantly inhibit the growth of the K562 cells. As shown in Fig. 5, A and B, neither O3OH nor S4OH had much effect on the doxorubicin IC_{50} value. O3OH increased the doxorubicin IC_{50} value from 0.065 to 0.14 μM, whereas S4OH decreased it 0.017 μM. Thus, it can be concluded that neither of these bisphenols antagonized doxorubicin-induced growth inhibition of K562 cells through their ability to inhibit topoisomerase IIα.

The ability of 300 μM DHDP (a weaker topoisomerase IIα inhibitor) and S4OH to antagonize etoposide-induced growth inhibition of K562 cells was also evaluated. A 30-min pretreatment with the bisphenol was followed by a 1-h treatment with etoposide, after which both drugs were washed off. The concentrations of DHDP and S4OH were sufficiently high to strongly inhibit the catalytic activity of topoisomerase IIα (10- and 400-fold above the IC_{50} for catalytic activity inhibition, respectively; Table 1). As shown in Fig. 5C, DHDP increased the etoposide IC_{50} value nearly 6-fold from 17 to 97 μM, indicating that it antagonized the growth inhibitory effects of etoposide. However, as shown in Fig. 5D, S4OH, as with the doxorubicin treatment, had little effect, because it

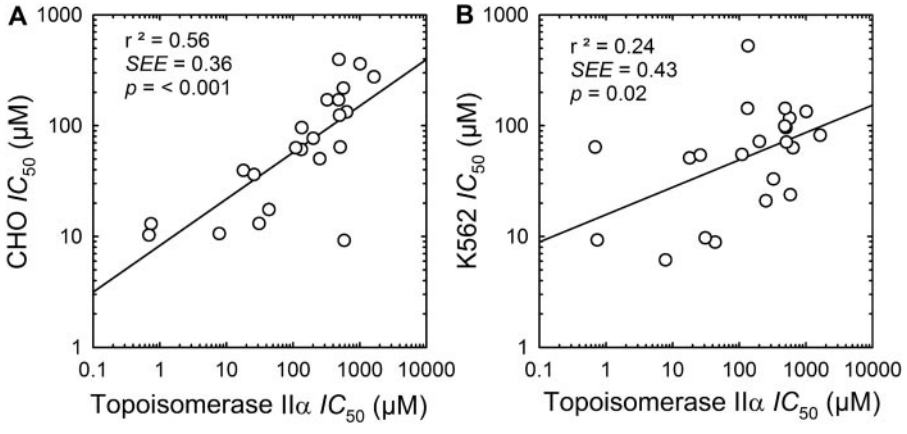

Fig. 3. Correlations of growth inhibition of CHO and K562 cells with inhibition of topoisomerase IIα by the bisphenols. A, correlation of the IC_{50} value for growth inhibition of CHO cells with the IC_{50} value for the inhibition of topoisomerase IIα. B, correlation of the IC_{50} value for growth inhibition of K562 cells with the IC_{50} value for the inhibition of topoisomerase IIα. The data are plotted on both axes with logarithmic scales. The straight lines were calculated from a linear least-squares analysis.

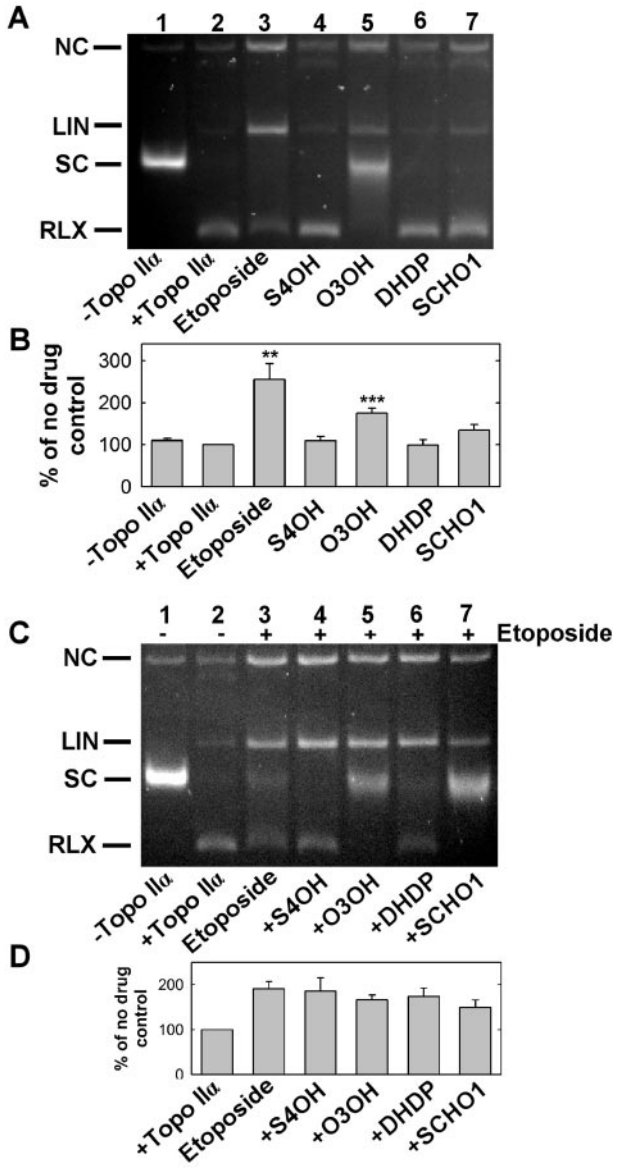

Fig. 4. Effect of bisphenols on the topoisomerase IIα-mediated relaxation and cleavage of supercoiled pBR322 DNA and their inhibition of etoposide-induced DNA cleavage. A, this typical fluorescent image of gels run in the presence of ethidium bromide shows the ability of the bisphenols to produce linear DNA above control levels (lane 1). As shown in lane 3, etoposide treatment produced linear DNA (LIN). In this gel, the relaxed DNA (RLX) ran ahead of the supercoiled DNA (SC). Topoisomerase IIα was present in the reaction mixture in all lanes but lane 1. B, bar graph of average ± S.E.M. integrated band intensity values for linear DNA for the compounds in A. Only etoposide (lane 3; **, $p < 0.01$) and O3OH (lane 5; ***, $p < 0.001$) significantly induced formation of linear DNA compared with control (lane 1). None of the other bisphenols tested produced significant amounts of linear DNA, indicating that they were not topoisomerase IIα poisons. The error bars are calculated from replicates from five determinations on different days. The bisphenols and etoposide were present at 250 μM. Topo IIα is topoisomerase IIα. C, this typical fluorescent image of gels run in the presence of ethidium bromide shows the effect of the bisphenols (lanes 4–7) on etoposide-induced formation of linear DNA (lane 3). Where indicated the bisphenols and etoposide were present at 100 μM. D, bar graph of the average ± S.E.M. integrated band intensities for the linear DNA band for the compounds tested in C. Etoposide produced an average 1.9-fold increase in linear DNA compared with the no-drug control (lane 1). Although all of the bisphenols decreased the amount of linear DNA, none of these decreases achieved statistical significance compared with etoposide-only induced formation of linear DNA. The error bars are calculated from four replicate determinations on different days.

decreased the IC_{50} value only slightly to 12 μM. A similar attempt was made to evaluate O3OH (30 μM) and SCHO1 (200 μM). However, these compounds could not be evaluated, because even after removal of drugs by washing, both these drugs were growth inhibitory (data not shown), probably as a result of retained drug.

3D-QSAR Modeling Based on the Inhibition of the Decatenation Activity of Topoisomerase IIα and the Growth Inhibition of K562 Cells. The wide range of topoisomerase IIα inhibitory IC_{50} values allowed us to carry out 3D-QSAR CoMFA and CoMSIA analyses to identify the structural features responsible for the inhibitory activity of the bisphenol compounds. The energy-minimized structure of OCHO2 (Fig. 6A) was selected as the template molecule, because it had *meta*- and *para*-substituents on both phenyl

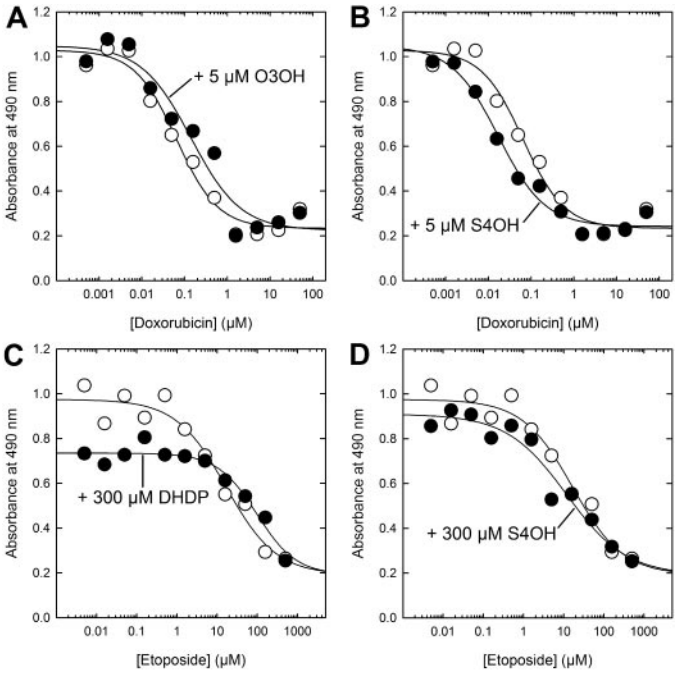

Fig. 5. Effect of preincubation of K562 cells with bisphenol topoisomerase IIα catalytic inhibitors. A, K562 cells were either untreated (○) or pretreated (●) with 5 μM O3OH for 30 min before treatment with doxorubicin for 72 h before assessment of growth inhibition by an MTS assay. The curved solid lines are nonlinear least-squares fits to a four-parameter logistic equation, and they yield IC_{50} values of 0.065 ± 0.022 and 0.142 ± 0.008 μM, respectively, for no pretreatment and pretreatment with 5 μM O3OH. B, K562 cells were either untreated (○) or pretreated (●) with 5 μM S4OH for 30 min before treatment with doxorubicin for 72 h before assessment of growth inhibition by an MTS assay. The curved solid lines are nonlinear least-squares fits to a four-parameter logistic equation, and they yield an IC_{50} value of 0.0017 ± 0.006 μM for pretreatment with 5 μM O3OH. The concentration of 5 μM O3OH or S4OH is approximately 6-fold higher than that required to inhibit the catalytic activity of topoisomerase IIα. Neither O3OH nor S4OH antagonized the growth inhibitory effects of doxorubicin. C, K562 cells were either untreated (○) or pretreated (●) with 300 μM DHDP for 30 min before a 1-h treatment with etoposide, after which both drugs were washed off. After 72 h, growth inhibition was assessed by an MTS assay. The curved solid lines are nonlinear least-squares fits to a logistic equation, and they yield IC_{50} values of 17 ± 11 and 97 ± 22 μM, respectively, for no pretreatment and pretreatment with 300 μM DHDP. D, K562 cells were either untreated (○) or pretreated (●) with 300 μM S4OH for 30 min before a 1-h treatment with etoposide. After 72 h, growth inhibition was assessed by an MTS assay. The curved solid lines are nonlinear least-squares fits to a four-parameter logistic equation. The IC_{50} value is 12 ± 10 μM for pretreatment with 300 μM S4OH. The concentration of 300 μM DHDP or S4OH was much higher than that required to inhibit the catalytic activity of topoisomerase IIα.

rings and thus would occupy 3D space common to many of the bisphenols of Fig. 1. The other compounds in the data set were prepared by modifying the structure of OCHO2 and energy minimizing all but the aromatic carbon atoms (Fig. 6A). The resulting aligned structures are shown in Fig. 6B. The results of the CoMFA and CoMSIA analyses of the IC_{50} data for the inhibition of the topoisomerase IIα are summarized in Table 2. Weakly inhibiting bisphenols, with an IC_{50} value larger than 570 μM, were not included in the analyses due to inaccuracies in determining these values. No compound was found to be an outlier in the CoMFA analyses. However, S3OH was found to be an outlier in the CoMSIA analysis. Due to the relatively small numbers of compounds in each data set (19 and 18, respectively) all structures were used in the analyses, rather than dividing them into training and validation sets. The predicted and experimental pIC_{50} values for the CoMFA and CoMSIA analyses for inhibition of topoisomerase IIα and K562 cell growth inhibition are plotted in Fig. 7, A to C, respectively. The CoMSIA analysis was well correlated, with an r^2 value of 0.90 and a moderately good q^2 value of 0.46. However, the CoMFA analysis did not yield good r^2 or q^2 values. The CoMSIA analysis for the inhibition of the topoisomerase IIα likely yielded a better model because, in addition to the steric and electrostatic contributions to the field, CoMSIA also measures hydrophobic and hydrogen bond donor and acceptor contributions to the field; thus, it provides a more complete description of the interaction of the molecules with its binding site. The electrostatic contribution to the CoMSIA-derived field at 31.7% was the largest contributor to the overall field (Table 2). The hydrogen bond acceptor and hydrogen bond acceptor components at 25.2 and 23.7%, respectively, were the second and third largest contributors to the field (Table 2).

An examination of the four isocontour diagrams ("stdev*coeff"; Fig. 6C–F) for the four largest field components for inhibition of topoisomerase IIα that were mapped onto the OCHO2 molecule shows the regions in space that were either favored or disfavored for inhibitory activity. The green contours indicate regions that increased inhibitory activity, and the red contours indicate regions that decreased inhibitory activity. An examination of the electrostatic field, which makes the largest contribution to the CoMSIA-derived field, showed that bisphenol analogs with polar substituents such as hydroxyl groups in the meta-position on the phenyl rings were favored. For the hydrogen bond acceptor field, the second largest contributor to the CoMSIA-derived field, a *meta*-substituted heteroatom, as in a hydroxyl or formyl group was favored, whereas the sulfoxide or sulfone oxygens on the bridge were disfavored. For the hydrogen bond donor field *para*-and *meta*-substituted hydroxyl groups were favored. For the hydrophobic field, the region around the bridge atom was disfavored, which probably reflects the higher hydrophobicity of the alkyl substituents in this region.

CoMFA and CoMSIA analyses was also carried out on the IC_{50} data for K562 and K/VP.5 cell growth inhibition for the 23 bisphenols in Table 1. The CoMSIA analysis yielded q^2 values of 0.29 and 0.55, respectively, but with six and seven optimum components, respectively (Table 3). The r^2 values of 0.91 and 0.97, respectively, were quite good. The predicted and experimental pIC_{50} values for the CoMFA and CoMSIA analyses are plotted in Fig. 7, C and D, for the K562 cells. The electrostatic and hydrogen bond acceptor terms, respectively, made the largest contribution to the overall field, similar to what was found for the topoisomerase II CoMSIA analysis, as might be expected given that their activities are correlated

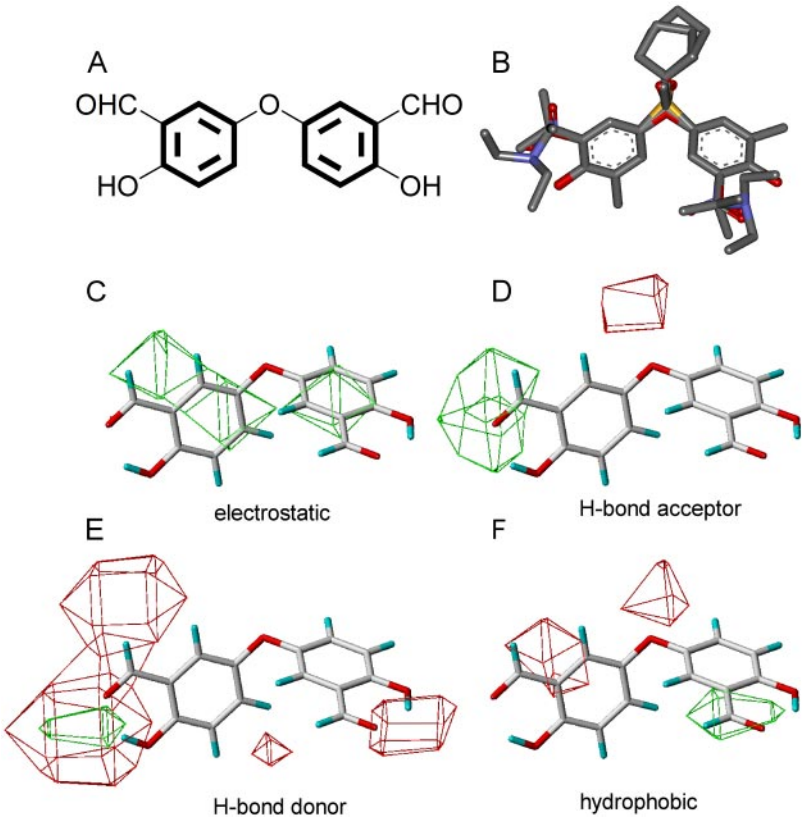

Fig. 6. A, structure of OCHO2 that was used as a template molecule in the 3D-QSAR modeling for the inhibition of topoisomerase IIα. The atoms connecting the bonds in bold were used for the molecular alignments in the CoMFA and CoMSIA analyses. B, structures of 23 bisphenol energy-minimized structures aligned to the template molecule OCHO2 used in the 3D-QSAR modeling. Electrostatic (C), H-bond acceptor (D), H-bond donor (E), and hydrophobic stddev*coeff (F) contour maps superimposed on the structure of OCHOH2 obtained from the CoMSIA modeling for the topoisomerase IIα inhibitory activity of 18 bisphenols. In this order, these were the four most important field components that resulted from the CoMSIA modeling. The green grids outline the regions in space for each field that were favored for topoisomerase IIα inhibition, whereas the red areas show the regions that were disfavored.

(Fig. 3). As with the topoisomerase IIα data, the CoMFA analysis did not yield high r^2 or q^2 values.

Discussion

After the identification of DHDP as a new lead bisphenol compound from the National Cancer Institute database with good topoisomerase IIα inhibitory activity, a series of bisphenol analogs were prepared and tested to identify the structural features that were responsible for their activity. The bisphenols represent a new structural class of catalytic topoisomerase II inhibitors. Some of the bisphenols potently inhibited the growth of CHO and K562 cells in the low micromolar range. The fact that cell growth inhibition of CHO and K562 cells was positively correlated with topoisomerase IIα inhibition ($p < 0.001$ and 0.02, respectively, and an r^2 of 0.56 and 0.24, respectively) suggests that the catalytic inhibition of topoisomerase II contributed to the growth inhibitory activity, even though it may not have been the only mechanism by which these compounds acted. This correlation can be compared with a previous QSAR study in which we showed that a series of 12 bisdioxopiperazines, that included dexrazoxane (ICRF-187) and ICRF-193, that the logarithm of the CHO IC_{50} was correlated with the catalytic inhibition of topoisomerase II, with an $r^2 = 0.74$ and a $p = 0.0003$ (Hasinoff et al., 1995). As a group, the bisdioxopiperazines may only target topoisomerase II, whereas the bisphenols may also have inhibited cell growth through other mechanisms involving other targets and also possibly through cytotoxic metabolites.

Of the bisphenols tested, only O3OH significantly induced formation of linear DNA. Thus, O3OH may act, in part, as a topoisomerase IIα poison. Although O3OH and S4OH were equipotent in their ability to inhibit the decatenation activity of topoisomerase IIα (Table 1), only the former induced significant topoisomerase IIα-mediated cleavage of DNA (Fig. 4, A and B). This is analogous to the situation with doxorubicin and aclarubicin, two structurally similar anthracyclines that differ only in their sugar residue, in which only the former is a topoisomerase II poison (Larsen et al., 2003). Most bisphenols were not cross-resistant, or they were only low-fold cross-resistant, to the K/VP.5 cell line containing reduced levels of topoisomerase IIα and topoisomerase IIβ (Ritke et al., 1994a,b). These results suggest that most of the bisphenols exerted their activity as catalytic inhibitors of topoisomerase II, but that they did not act as topoisomerase II poisons. Topoisomerase II catalytic inhibitors such as the bisdioxopiperazines dexrazoxane and ICRF-193 (Sehested et al., 1993; Hasinoff et al., 1996) and a newly identified "purine class" (NSC35866) of compounds (Jensen et al., 2005) can antagonize the growth inhibitory effects of topoisomerase II poisons. However, not all of the purines acted like NSC35866, because our follow-up study showed that most of the purines were not capable of antagonizing etoposide-induced cytotoxicity and DNA strand breaks in cells (Jensen et al., 2006).

TABLE 2
Partial least-squares statistics and field contributions from CoMFA and CoMSIA models for the prediction of pIC_{50} values for the inhibition of topoisomerase IIα
q^2 is the LOO cross-validated correlation coefficient, N is optimum number of components, and r^2 is the noncross-validated correlation coefficient.

Parameter	CoMFA	CoMSIA
q^2	0.076	0.463
N	1	4
Standard error of prediction	0.950	0.827
r^2	0.306	0.895
Standard error of the estimate	0.823	0.365
F-test value	7.512	27.750
Field contributions		
Steric	0.464	0.044
Electrostatic	0.536	0.317
Hydrophobic		0.150
Hydrogen bond donor		0.237
Hydrogen bond acceptor		0.252

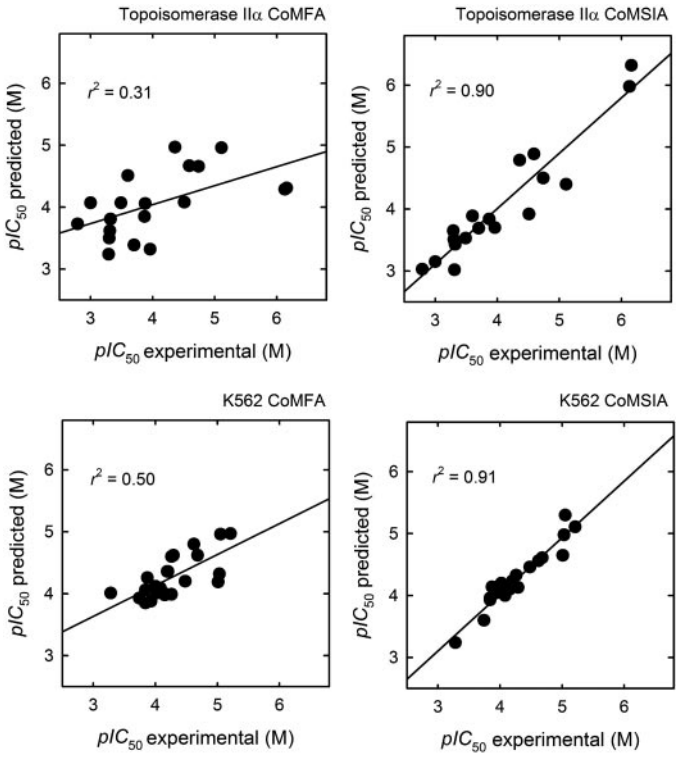

Fig. 7. A and B, correlation of the predicted and experimentally determined values of pIC_{50} for inhibition of the decatenation activity of topoisomerase IIα by the bisphenol analogs used in the building of the CoMFA and CoMSIA models, respectively. C and D, correlation of the predicted and experimentally determined values of pIC_{50} for inhibition of the K562 cell growth by the bisphenol analogs used in the building of the CoMFA and CoMSIA models, respectively. The straight lines were calculated from a linear least-squares analysis.

TABLE 3
Partial least-squares statistics and field contributions from CoMFA and CoMSIA models for the prediction of pIC_{50} values for the inhibition of the growth of K562 and K/VP.5 cells
q^2 is LOO cross-validated correlation coefficient, N is optimum number of components, and r^2 is non–cross-validated correlation coefficient.

Parameter	K562		K/VP.5	
	CoMFA	CoMSIA	CoMFA	CoMSIA
q^2	0.335	0.291	0.573	0.554
N	1	6	2	7
Standard error of prediction	0.401	0.474	0.358	0.423
r^2	0.499	0.913	0.754	0.965
Standard error of the estimate	0.348	0.166	0.272	0.118
F-test value	20.898	27.864	30.607	59.519
Field contributions				
Steric	0.265	0.082	0.310	0.067
Electrostatic	0.735	0.332	0.690	0.370
Hydrophobic		0.203		0.143
Hydrogen bond donor		0.144		0.134
Hydrogen bond acceptor		0.239		0.286

Although S4OH, O3OH, DHDP, and SCHO1 did decrease etoposide-induced linear DNA formation by purified topoisomerase IIα (Fig. 4, C and D), these decreases did not achieve statistical significance. Consistent with these results, the bisphenols S4OH and O3OH did not antagonize the K562 cell growth inhibitory effects of the topoisomerase II poison doxorubicin or etoposide (Fig. 5, A, B, and D), although, in contrast, DHDP did antagonize the growth inhibitory effects of etoposide (Fig. 5C). These results suggest subtle differences in the way that the bisphenols interacted with topoisomerase II. In addition, interference with doxorubicin activity may have been complicated by other mechanisms of growth inhibition such as generation of reactive oxygen species (Gewirtz, 1999). The lack of cross-resistance (Table 1) with the bisdioxopiperazine-resistant DZR cell line indicates that in spite of some general structural similarities, the bisphenols did not interact with the bisdioxopiperazine binding site of topoisomerase IIα.

To further define the structural factors that result in high cell growth inhibitory potency and topoisomerase IIα inhibitory activity for the bisphenols, 3D-QSAR CoMFA and CoMSIA analyses were carried out to derive a model for the prediction of activity to aid in the synthesis of new and more active analogs. Based on a common substructure alignment (Fig. 6, A and B), only the CoMSIA analyses for the topoisomerase IIα inhibitory activity gave a high-quality model based on its q^2 value (Table 2). The largest contributors to the CoMSIA field were electrostatic, hydrogen bond acceptor, hydrogen bond donor, hydrophobic and steric contributions, in that order. Mapping of these fields (Fig. 6) onto the structure of OCHO2, one of the most cytotoxic bisphenols, showed that for both the electrostatic and hydrogen bond acceptor fields, bisphenol analogs with a hydroxyl or formyl group in the *meta*-position on the phenyl rings favored increased topoisomerase IIα inhibitory activity. However, the sulfoxide or sulfone oxygens on the bridge were disfavored. Polar *meta*-hydrogen bond acceptor substituents on the phenyl rings also favored inhibition of topoisomerase IIα.

In summary, a series of bisphenol compounds were identified that were catalytic inhibitors of topoisomerase II. Thus, it is likely that the bisphenols exerted their cell growth inhibitory activity, in part, through their ability to inhibit topoisomerase IIα. Of the bisphenols tested, only O3OH induced significant topoisomerase IIα-mediated cleavage of DNA. Forward development of these compounds or their analogs as clinically useful topoisomerase II targeting agents is supported by the results presented. If these bisphenols are able to antagonize etoposide-induced cleavable complex formation, then these compounds may be clinically useful in preventing systemic toxicity while targeting brain cancer tumors with high-dose therapy with topoisomerase II poisons, as has been suggested for dexrazoxane in previous reports (Jensen and Sehested, 1997a,b; Holm et al., 1998).

References

Akimitsu N, Adachi N, Hirai H, Hossain MS, Hamamoto H, Kobayashi M, Aratani Y, Koyama H, and Sekimizu K (2003) Enforced cytokinesis without complete nuclear division in embryonic cells depleting the activity of DNA topoisomerase IIα. *Genes Cells* **8:**393–402.

Andoh T and Ishida R (1998) Catalytic inhibitors of topoisomerase II. *Biochim Biophys Acta* **1400:**155–171.

Burden DA, Froelich-Ammon SJ, and Osheroff N (2001) Topoisomerase II-mediated cleavage of plasmid DNA. *Methods Mol Biol* **95:**283–289.

Classen S, Olland S, and Berger JM (2003) Structure of the topoisomerase II ATPase region and its mechanism of inhibition by the chemotherapeutic agent ICRF-187 [published erratum appears in *Proc Natl Acad Sci U S A* **100:**14510, 2003]. *Proc Natl Acad Sci U S A* **100:**10629–10634.

Cramer RD 3rd, Patterson DE, and Bunce JD (1988) Comparative molecular field analysis (CoMFA). 1. Effect of shape on binding of steroids to carrier proteins. *J Am Chem Soc* **110:**5959–5967.

Fattman C, Allan WP, Hasinoff BB, and Yalowich JC (1996) Collateral sensitivity to the bisdioxopiperazine dexrazoxane (ICRF-187) in etoposide (VP-16) resistant human leukemia K562 cells. *Biochem Pharmacol* **52:**635–642.

Fortune JM and Osheroff N (2000) Topoisomerase II as a target for anticancer drugs: when enzymes stop being nice. *Prog Nucleic Acid Res Mol Biol* **64:**221–253.

Gewirtz DA (1999) A critical evaluation of the mechanisms of action proposed for the antitumor effects of the anthracycline antibiotics adriamycin and daunorubicin. *Biochem Pharmacol* **57:**727–741.

Hasinoff BB, Kuschak TI, Creighton AM, Fattman CL, Allan WP, Thampatty P, and Yalowich JC (1997) Characterization of a Chinese hamster ovary cell line with acquired resistance to the bisdioxopiperazine dexrazoxane (ICRF-187) catalytic inhibitor of topoisomerase II. *Biochem Pharmacol* **53:**1843–1853.

Hasinoff BB, Kuschak TI, Yalowich JC, and Creighton AM (1995) A QSAR study comparing the cytotoxicity and DNA topoisomerase II inhibitory effects of bisdioxopiperazine analogs of ICRF-187 (dexrazoxane). *Biochem Pharmacol* **50:**953–958.

Hasinoff BB, Wu X, Begleiter A, Guziec L, Guziec F, Giorgianni A, Yang S, Jiang Y, and Yalowich JC (2006) Structure-activity study of the interaction of bioreductive benzoquinone alkylating agents with DNA topoisomerase II. *Cancer Chemother Pharmacol* **57:**221–233.

Hasinoff BB, Wu X, Krokhin OV, Ens W, Standing KG, Nitiss JL, Sivaram T, Giorgianni A, Yang S, Jiang Y, et al. (2005) Biochemical and proteomics approaches to characterize topoisomerase IIα cysteines and DNA as targets responsible for cisplatin-induced inhibition of topoisomerase IIα. *Mol Pharmacol* **67:**937–947.

Hasinoff BB, Wu X, and Yang Y (2004) Synthesis and characterization of the biological activity of the cisplatin analogs, *cis*-$PtCl_2$(dexrazoxane) and *cis*-$PtCl_2$(levrazoxane), of the topoisomerase II inhibitors dexrazoxane (ICRF-187) and levrazoxane (ICRF-186). *J Inorg Biochem* **98:**616–624.

Hasinoff BB, Yalowich JC, Ling Y, and Buss JL (1996) The effect of dexrazoxane (ICRF-187) on doxorubicin- and daunorubicin-mediated growth inhibition of Chinese hamster ovary cells. *Anticancer Drugs* **7:**558–567.

Holm B, Sehested M, and Jensen PB (1998) Improved targeting of brain tumors using dexrazoxane rescue of topoisomerase II combined with supralethal doses of etoposide and teniposide. *Clin Cancer Res* **4:**1367–1373.

Ishida R, Miki T, Narita T, Yui R, Sato M, Utsumi KR, Tanabe K, and Andoh T (1991) Inhibition of intracellular topoisomerase II by antitumor bis(2,6-dioxopiperazine) derivatives: mode of cell growth inhibition distinct from that of cleavable complex-forming type inhibitors. *Cancer Res* **51:**4909–4916.

Jensen LH, Liang H, Shoemaker RH, Grauslund M, Sehested M, and Hasinoff BB (2006) A three-dimensional quantitative structure-activity relationship study of the inhibition of the ATPase activity and the strand passing catalytic activity of topoisomerase IIα by substituted purine analogs. *Mol Pharmacol* **70:**1503–1513.

Jensen LH, Thougaard AV, Grauslund M, Sokilde B, Carstensen EV, Dvinge HK, Scudiero DA, Jensen PB, Shoemaker RH, and Sehested M (2005) Substituted purine analogues define a novel structural class of catalytic topoisomerase II inhibitors. *Cancer Res* **65:**7470–7477.

Jensen PB and Sehested M (1997a) DNA topoisomerase II rescue by catalytic inhibitors. *Biochem Pharmacol* **54:**755–759.

Jensen PB and Sehested M (1997b) DNA topoisomerase II rescue by catalytic inhibitors: a new strategy to improve the antitumor selectivity of etoposide. *Biochem Pharmacol* **54:**755–759.

Klebe G, Abraham U, and Mietzner T (1994) Molecular similarity indices in a comparative analysis (CoMSIA) of drug molecules to correlate and predict their biological activity. *J Med Chem* **37:**4130–4146.

Kubinyi H, Hamprecht FA, and Mietzner T (1998) Three-dimensional quantitative similarity-activity relationships (3D QSiAR) from SEAL similarity matrices. *J Med Chem* **41:**2553–2564.

Larsen AK, Escargueil AE, and Skladanowski A (2003) Catalytic topoisomerase II inhibitors in cancer therapy. *Pharmacol Ther* **99:**167–181.

Li TK and Liu LF (2001) Tumor cell death induced by topoisomerase-targeting drugs. *Annu Rev Pharmacol Toxicol* **41:**53–77.

Liang H, Wu X, Guziec LJ, Guziec FSJ, Larson KK, Lang J, Yalowich JC, and Hasinoff BB (2006) A structure-based 3D-QSAR study of anthrapyrazole analogs of the anticancer agents losoxantrone and piroxantrone. *J Chem Inf Model* **46:**1827–1835.

Pommier Y, Pourquier P, Fan Y, and Strumberg D (1998) Mechanism of action of eukaryotic DNA topoisomerase I and drugs targeted to the enzyme. *Biochim Biophys Acta* **1400:**83–106.

Priebe W, Fokt I, Przewloka T, Chaires JB, Portugal J, and Trent JO (2001) Exploiting anthracycline scaffold for designing DNA-targeting agents. *Methods Enzymol* **340:**529–555.

Ritke MK, Allan WP, Fattman C, Gunduz NN, and Yalowich JC (1994a) Reduced phosphorylation of topoisomerase II in etoposide-resistant human leukemia K562 cells. *Mol Pharmacol* **46:**58–66.

Ritke MK, Roberts D, Allan WP, Raymond J, Bergoltz VV, and Yalowich JC (1994b) Altered stability of etoposide-induced topoisomerase II-DNA complexes in resistant human leukaemia K562 cells. *Br J Cancer* **69:**687–697.

Sehested M, Jensen PB, Sorensen BS, Holm B, Friche E, and Demant EJF (1993) Antagonistic effect of the cardioprotector (+)-1,2-bis(3,5-dioxopiperazinyl-1-

yl)propane (ICRF-187) on DNA breaks and cytotoxicity induced by the topoisomerase II directed drugs daunorubicin and etoposide (VP-16). *Biochem Pharmacol* **46:**389–393.
Tanabe K, Ikegami Y, Ishida R, and Andoh T (1991) Inhibition of topoisomerase II by antitumor agents bis(2,6-dioxopiperazine) derivatives. *Cancer Res* **51:** 4903–4908.
Wang JC (2002) Cellular roles of DNA topoisomerases: a molecular perspective. *Nat Rev Mol Cell Biol* **3:**430–440.
Wilstermann AM and Osheroff N (2003) Stabilization of eukaryotic topoisomerase II-DNA cleavage complexes. *Curr Top Med Chem* **3:**321–338.
Wu X and Hasinoff BB (2005) The antitumor anthracyclines doxorubicin and daunorubicin do not inhibit cell growth through the formation of iron-mediated reactive oxygen species. *Anticancer Drugs* **16:**93–99.
Zhang H, D'Arpa P, and Liu LF (1990) A model for tumor cell killing by topoisomerase poisons. *Cancer Cells* **2:**23–27.

Address correspondence to: Dr. Brian Hasinoff, Faculty of Pharmacy, University of Manitoba, Winnipeg, MB R3T 2N2, Canada. E-mail: b_hasinoff@umanitoba.ca